DYNAMIC ANALYSIS OF THE HUALIEN LARGE-SCALE CONTAINMENT MODEL

by

Todor Ganev[1], Fumio Yamazaki[2] and Tsuneo Katayama[3]

INTRODUCTION

The Hualien Large-Scale Seismic Test is an international project on dynamic soil-structure interaction. It is sponsored by a consortium of industrial and research enterprises from five countries (Japan, USA, Taiwan, France and Korea). The Hualien project has been initiated as a continuation of the Lotung Large-Scale Seismic Experiment (EPRI, 1987). Both test programs have involved construction of nuclear power plant containment models and monitoring of their earthquake response in conjunction with the surrounding soil. Hualien is located south of Lotung on the east coast of Taiwan, in a highly active seismic zone near the Phillipine Sea Plate boundary. The data recorded at both sites and the results of their analysis have proven very useful for verification of the existing theoretical and numerical approaches towards the problems of dynamic soil-structure interaction.

The Lotung Experiment has been carried out on soft soil. It has provided valuable data and insight into the complex interaction phenomena. In its turn, the Hualien Model has been constructed on stiff soil following the need to confirm and expand the findings of the previous program (Tang et al., 1991). It is of practical interest to compare the interaction effects, which occur at stiff and soft soil sites and to seek their integrated quantitative interpretations for analysis and design purposes.

The objective of this paper is to present results from forced vibration tests, microtremor observations and earthquake response analysis of the Hualien Model. The present authors have previously investigated the soil-structure interaction of a reinforced concrete tower, constructed on soft soil in Chiba, Japan. A comparison between the results of the two studies is offered.

DESCRIPTION OF THE MODEL AND THE EXPERIMENTAL DATA

The test structure represents a one-fourth scale model of a nuclear power containment. Its dimensions are shown in Figure 1. The depth of the embedment is 5 m, which consists 31% of the total height. The weight of the whole structure is 1440.2 tf (14128 kN). Forty-six per cent of the total mass is concentrated in the foundation and thirty-five per cent in the roof.

Accelerometers are installed at all points of interest on the structure, as illustrated in

1) Graduate student, Civil Engineering Department, University of Tokyo.
2) Associate Professor, Institute of Industrial Science, University of Tokyo.
3) Professor, ditto.

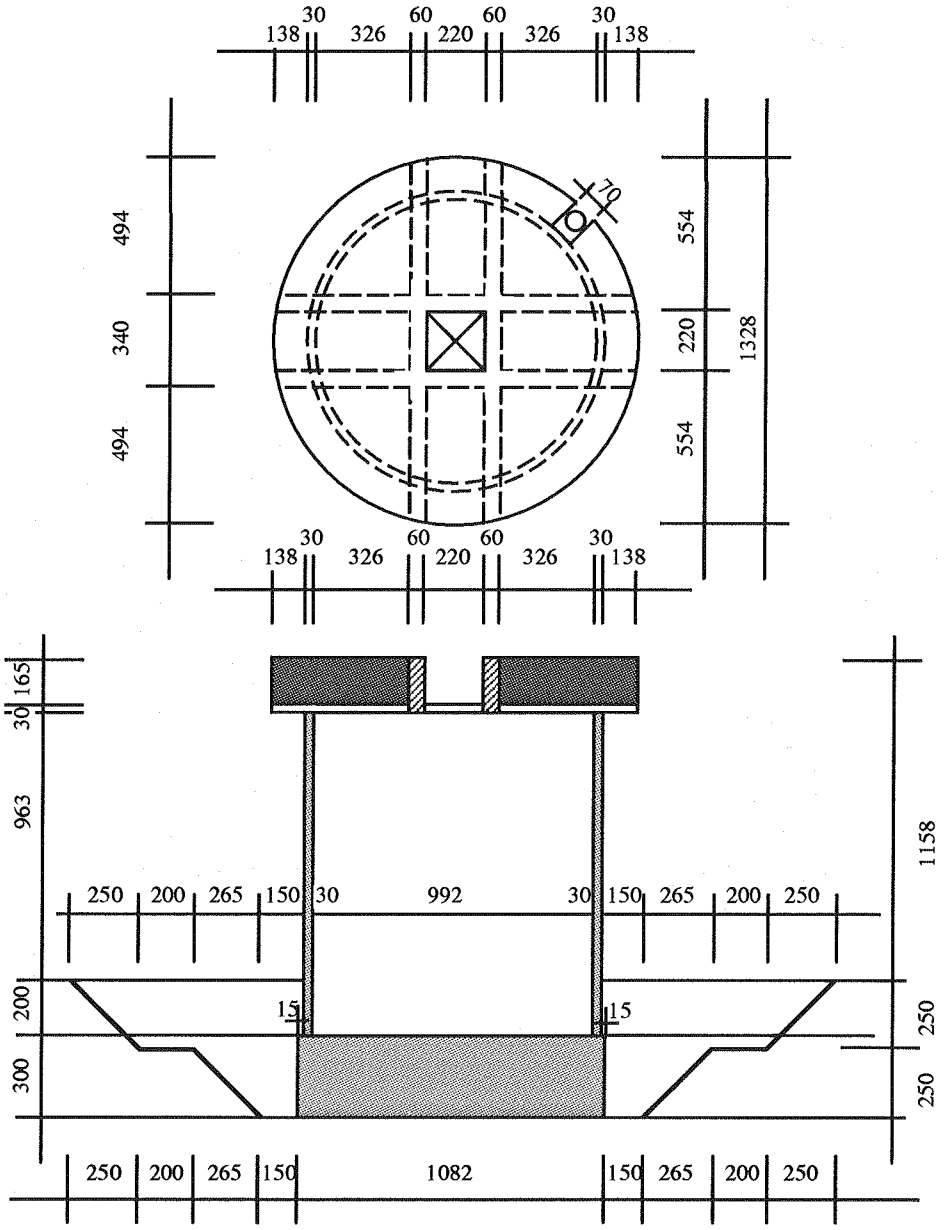

Figure 1. Plan and vertical cross-section of the containment model

Figure 2. Twenty-eight soil pressure transducers are attached to the embedded portion of the cylindrical wall and to the bottom of the foundation (Figure 3). Surface and downhole seismometers, monitoring the motion of the soil are arranged in a three dimensional array around the structure, as shown in Figure 4.

The properties of the soil around and beneath the structure have been systematically investigated by in-situ tests which comprise borings, large penetration tests and PS-loggings and laboratory tests which include triaxial tests on frozen undisturbed samples (Kokusho et al.,

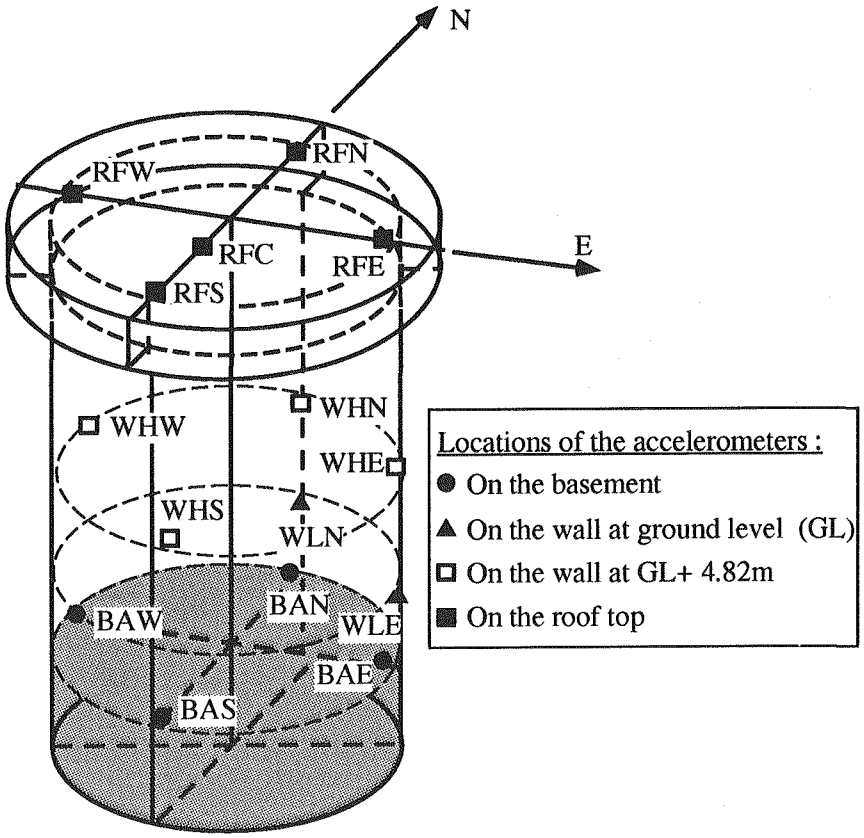

Figure 2. Locations of the accelerometers on the structure

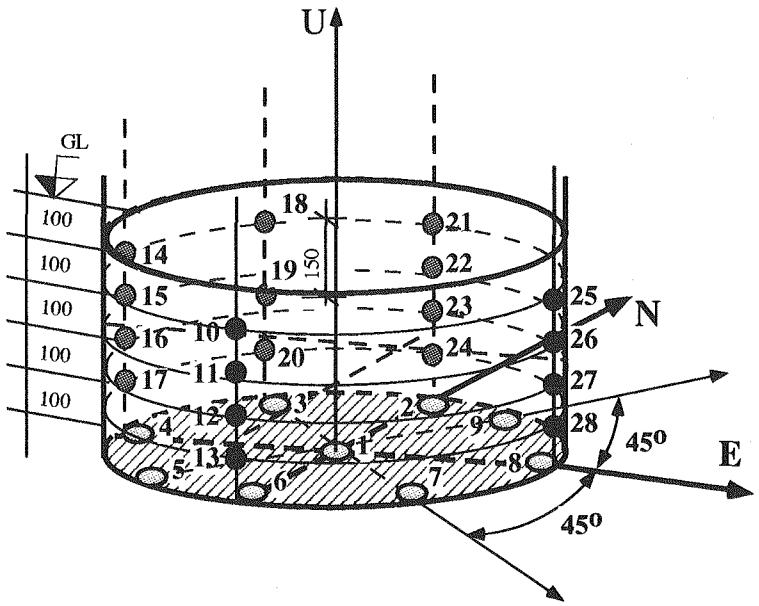

Figure 3. Locations of the soil-pressure gauges

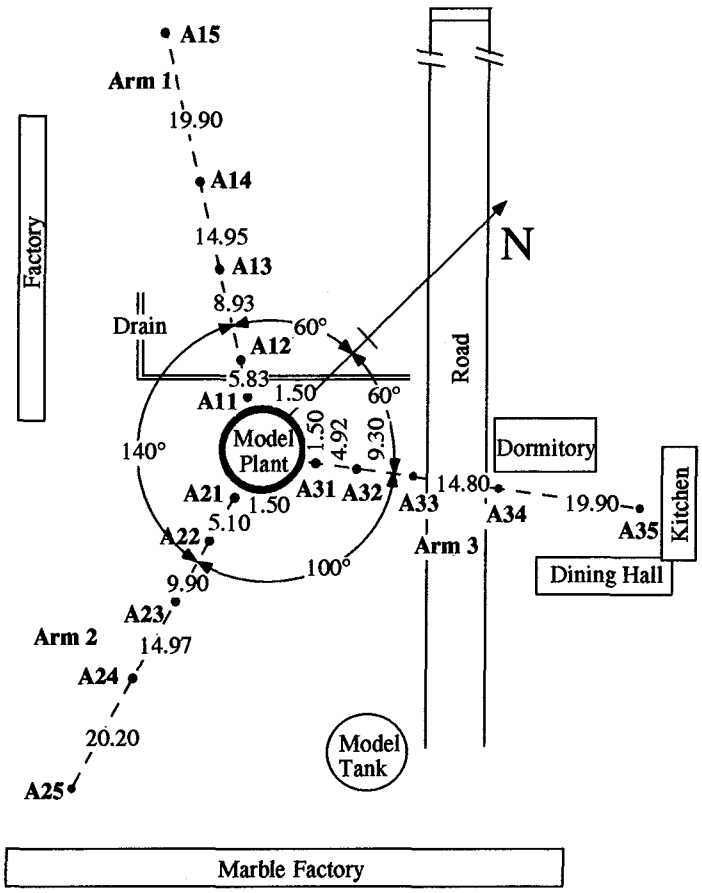

a) Plan of the site

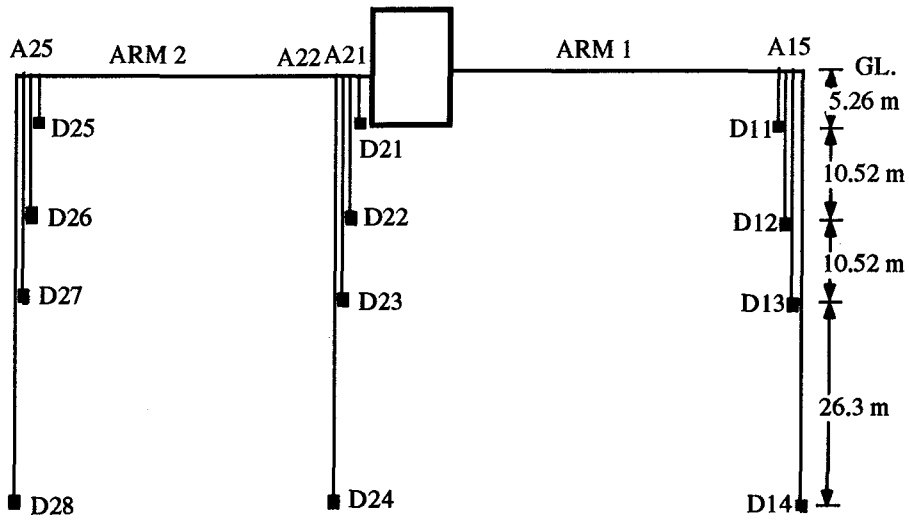

b) Vertical cross-section of the site

Figure 4. Locations of the accelerometers at the experimental site

1993). Based on the geotechnical investigation, the Central Research Institute of Electric Power Industry (CRIEPI), Japan, created a soil model of the foundation ground. This model was named "unified ground model" (Kokusho et al., 1994) and was used by all the participants in the Hualien Project. Subsequently, some of the soil properties were revised, following geotechnical investigations, performed by CRIEPI in October 1994 and a "modified ground model" was suggested. The unified model and its modification are presented in Figure 5.

Two forced vibration tests have been conducted on the Hualien model: in October 1992 before backfill (FVT-1) and in February 1993 after backfill (FVT-2). In October 1994, the present authors conducted a series of microtremor observations of the structure and the surrounding soil using eight velocity-type pickups simultaneously.

Ganev et al. (1995b) determined the orientation errors of the free field accelerometers on the basis of earthquake data by means of the maximum cross-correlation method (Yamazaki et al., 1992). It was established that the records of surface station A15, which had been often used as control motions for numerical analysis, need correction. Counterclockwise rotation by 13 degrees is recommended.

Before the backfill was completed, the excavation was flooded by heavy rains and its slopes partially collapsed. This is believed to have created anisotropic conditions in the vicinity of the foundation, which cause cross-axis coupling of the horizontal response of the structure.

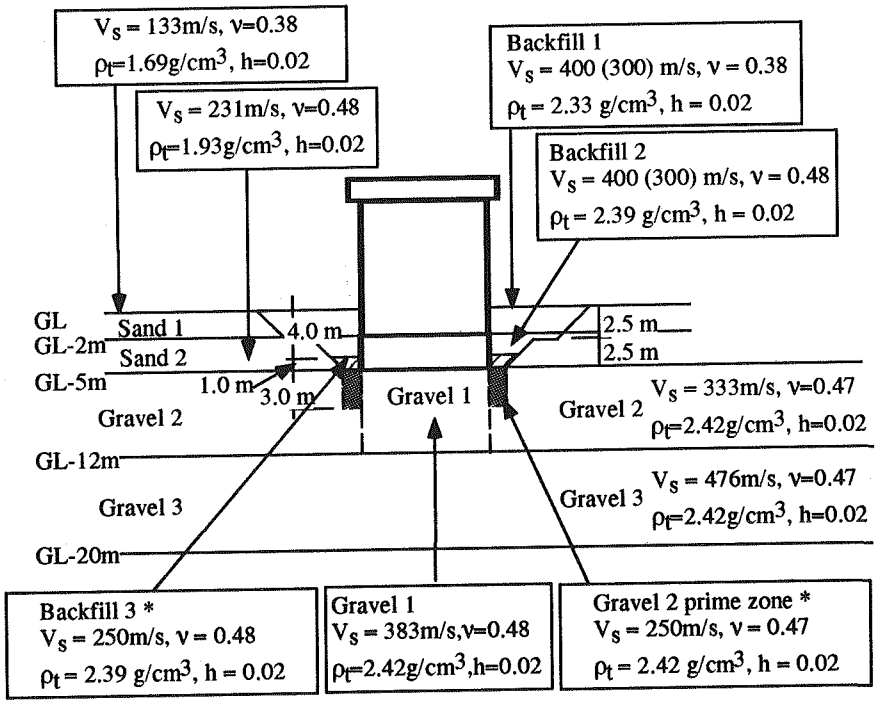

Notes:

Values in parentheses are those of the Modified Ground Model

Zones designated by * have been introduced in the Modified Ground Model

Figure 5. The Unified and Modified Ground Models (CRIEPI)

To minimize this effect, analysis can be conducted in the directions of the principal axes, which have been designated D1 and D2 (Morisita et al., 1993; Tanaka et al., 1994). Their position is found through rotating the geographical coordinate system counterclockwise by 61 degrees.

During the construction of the roof slab, twelve holes were made in the upper part of the shell wall, in order to insert temporary supporting beams for the formwork. Upon completion, the reinforcing bars were reconnected and the holes were filled, but the overall stiffness of the wall was rendered significantly lower than the initially intended.

Data from five earthquakes recorded at the Hualien site are used in this study. Basic information about the events is presented in Tables 1, 2 and 3.

Table 1. Earthquake events used in the analysis.

Event	Date mm/dd/yy	Epicenter		Magnitude
		Latitude	Longitude	
940120	01/20/94	24°03'36"N	121°51'00"E	5.6
940530	05/30/94	24°05'40"N	121°34'20"E	4.5
940605	06/05/94	24°27'60"N	121°50'40"E	6.2
950501	05/01/95	24°02'42"N	121°39'06"E	4.9
950502	05/02/95	24°00'44"N	121°38'24"E	4.6

Table 2. Peak acceleration (cm/s/s) at main points of interest.

Event	D1			D2		
	Ground	Basement	Roof	Ground	Basement	Roof
940120	36.65	30.22	79.47	26.56	24.93	55.09
940530	32.16	11.43	28.90	19.54	12.32	33.59
940605	24.52	24.58	61.77	28.11	22.66	52.39
950501	66.42	55.83	84.63	99.76	72.76	165.24
950502	38.56	26.12	72.72	58.43	22.74	64.46

Table 3. Peak velocity (cm/s) at main points of interest.

Event	D1			D2		
	Ground	Basement	Roof	Ground	Basement	Roof
940120	2.07	2.38	3.39	1.68	1.50	2.24
940530	0.90	0.69	0.93	0.67	0.65	1.10
940605	3.74	4.44	4.35	3.05	3.26	3.75
950501	5.01	4.93	5.73	5.83	5.48	7.90
950502	2.05	1.83	2.51	1.61	1.23	2.42

IDENTIFICATION OF SYSTEM CHARACTERISTICS

Figure 6 presents a formal comparison between the results of FVT-2 and a transfer function, evaluated from microtremor. The NS-direction is used for this illustration, because the microtremor observations in the North-South and East-West directions were carried out at different times and rotation to the principal axes would not be completely accurate. The predominant frequency of the system is identified as 6.4 Hz from FVT and 6.3 Hz from microtremor. This good agreement shows, that microtremor observation can be used successfully instead of forced vibration tests to evaluate system characteristics. Compared with the forced vibration tests, the microtremor observation is easy and inexpensive to perform. Also, from a theoretical point of view, microtremor is closer to earthquake excitation than FVT, and permits the same type of analysis.

Figure 7 shows Fourier spectrum ratios between the free field and the top of the structure, evaluated from earthquake records in the D2 direction. The predominant frequency of the system shifts from about 6.0 Hz for Event 940530 through 5.7 Hz for Event 940120 to 5.3 Hz for Event 950501. A similar phenomenon was observed previously by Ganev et al. (1995a) at a structure, built on soft soil. The reason for the shift of the predominant frequency is weakening of the soil support during earthquakes. This phenomenon usually can be explained with three factors: soil nonlinearity, separation of soil from the structure and pore water pressure buildup. At this point, no clear evidence of separation or pore water pressure buildup has been obtained. Most probably, the soil stiffness degradation under dynamic loads is due to highly nonlinear behavior as a result of local stress concentration at the contact with the foundation.

DYNAMIC ANALYSIS

Analysis of the structural response to FVT-2 was used as a starting point to establish suitable models for numerical simulation. The problem was approached in two different ways as described below.

Sway-Rocking Model

The behavior of the soil-structure system was simulated using the linear sway-rocking model shown in Figure 8. The values of the soil springs and dashpots were determined on the basis of the Continuum Formulation Method (CFM), developed by Harada et al., (1981). According to the provisions of the CFM, the sway spring K_H and dashpot C_H are to be evaluated for the whole embedment depth. In this case, however, while the stiffness of the massive fundament can be assumed infinite, it is recognized that the embedded part of the wall is deformable. This necessitates the division of the global K_H and C_H proportionally to the dimensions of each embedded part as illustrated in Figure 8.

At the time when the above described simulation was performed, the modified ground model had not yet been created. Soil properties according to the unified ground model (Figure 5) were used at the initial stage of this analysis.

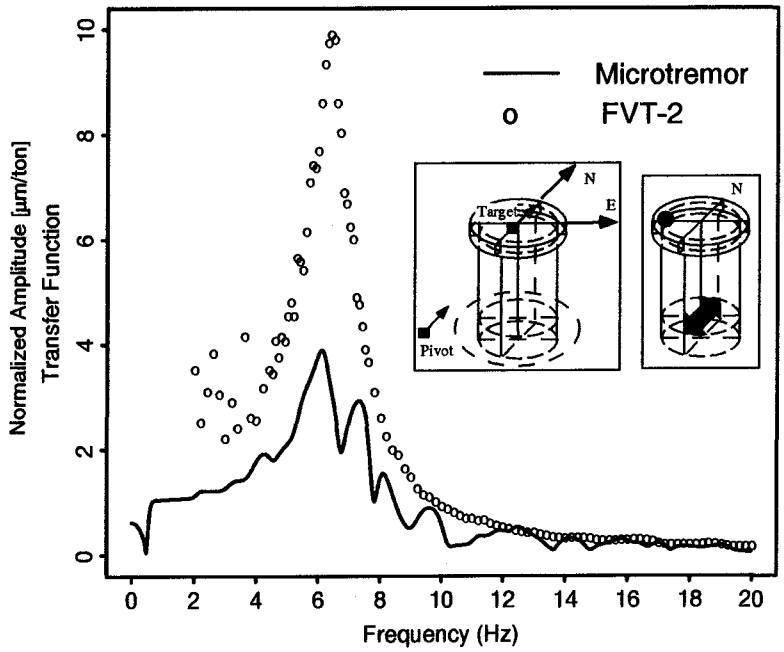

Figure 6. Formal comparison between FVT-2 (normalized amplitude) and microtremor(transfer function).

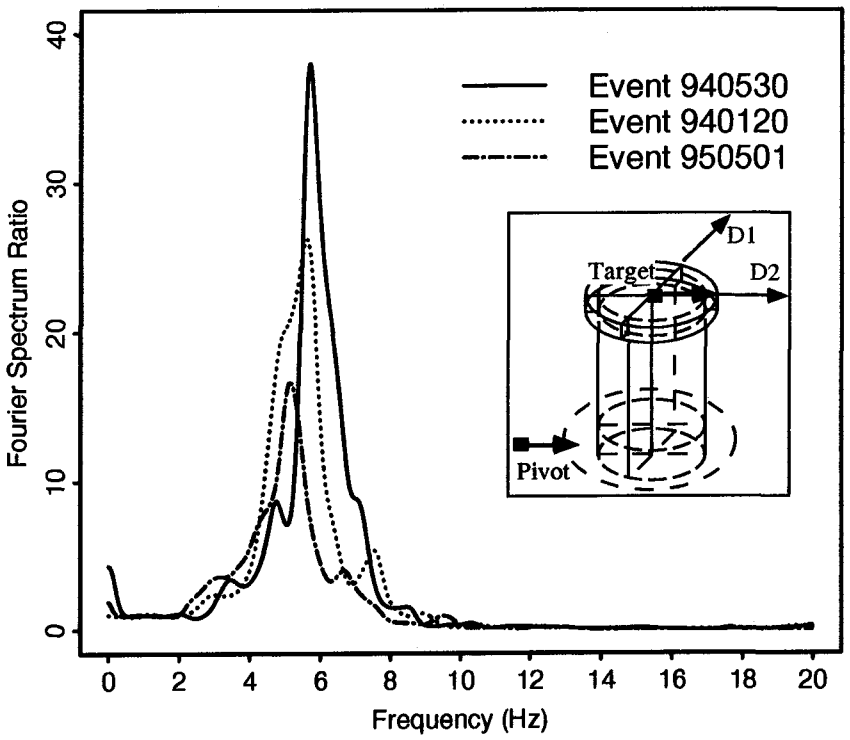

Figure 7. Fourier Spectrum ratios between the free field and the top of the structure

Finite Element Model (SASSI)

Alternatively, dynamic analysis was performed with the program SASSI employing the flexible volume substructuring approach (Lysmer et al., 1988). Taking advantage of the symmetry of the structure, a three-dimensional quarter model (Figure 9) was used, and slightly different properties of the layer below the foundation were considered for the D1 and D2 directions. A more detailed scheme of the finite element discretization is shown in Figure 10. By the time of this analysis, results of the latest geotechnical investigations performed by CRIEPI at the Hualien site were already available. Consequently, revised soil properties as prescribed by the modified ground model (Figure 5) were used for the finite element model.

At the initial stage, the properties of material types 5 and 7 (Figure 10) were assumed equal to type 4 in accordance with the assumption for existence of a softer annular region around the foundation walls (Veletsos and Dotson, 1988). Previous analysis of the forced vibration test by Tang and Nakamura (1995) has shown that this assumption leads to good results in the case of the Hualien model. The material properties used for simulation of response in D2- direction at the initial stage of the analysis can be seen in Table 4 in the column named "FVT".

The records at surface station A14 (Figure 4) were used as control motions for earthquake response analysis with both models.

RESULTS AND DISCUSSION

Dynamic response in the small strain range

Initially, the results of FVT-2, which represent small-strain linear behavior, were successfully simulated with both models. Figure 11 illustrates the good agreement between the recorded response and the two simulations. Subsequently, the models were validated by analyzing earthquake Event 940530, which had caused a very small relative structural response (c.f. Table 2) and no pronounced nonlinear effects. The simulations were successful.

As it has already been pointed out, due to the circumstances the CFM analysis was based on the unified ground model, while the modified model was employed in the SASSI analysis. Even though this is by itself an inconsistency, in view of the obtained results it provides some useful insight into the practice of numerical modeling. As can be seen in Figure 5, the backfills in the modified ground model have lower shear wave velocities and consequently lower stiffness than those of the unified model. The better accuracy of the Finite Element Method and the higher reliability of the modified ground model suggest that indeed, the backfills are softer than the initially stipulated in the unified ground model. The fact, that the sway-rocking model yielded the good agreement in Figure 11 despite this discrepancy, signifies that the Continuum Formulation Method tends to underestimate the soil stiffness.

The reason for this tendency is in the theoretical basis of the method. When evaluating soil reaction caused by rocking on a point on the wall of a cylindric foundation, the components of the stress tensor which act in the horizontal plane perpendicular to the axis of the cylinder are neglected for simplification (Harada et al., 1981, Appendix). In this way, some of the shear resistance of the soil is ignored.

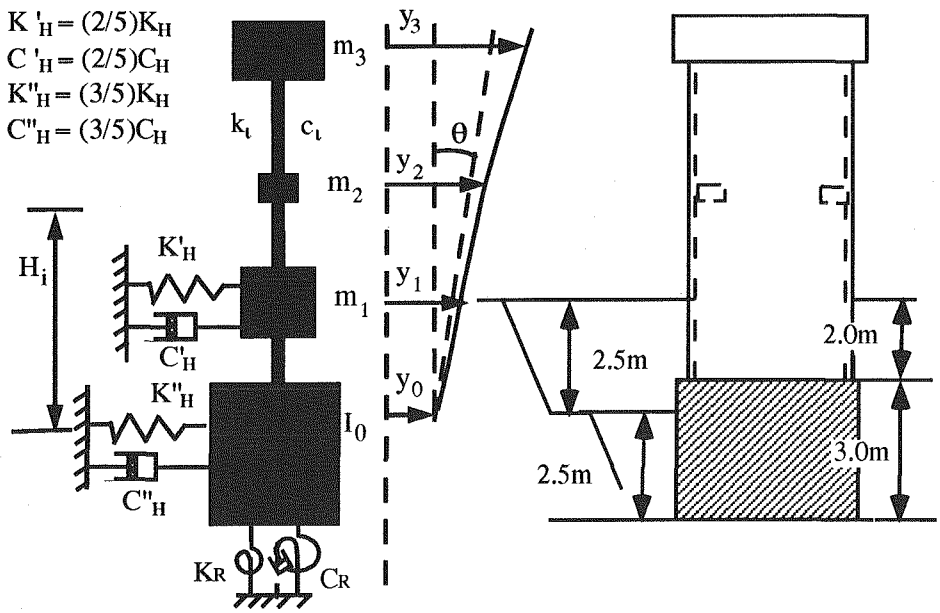

Figure 8. Sway-rocking model

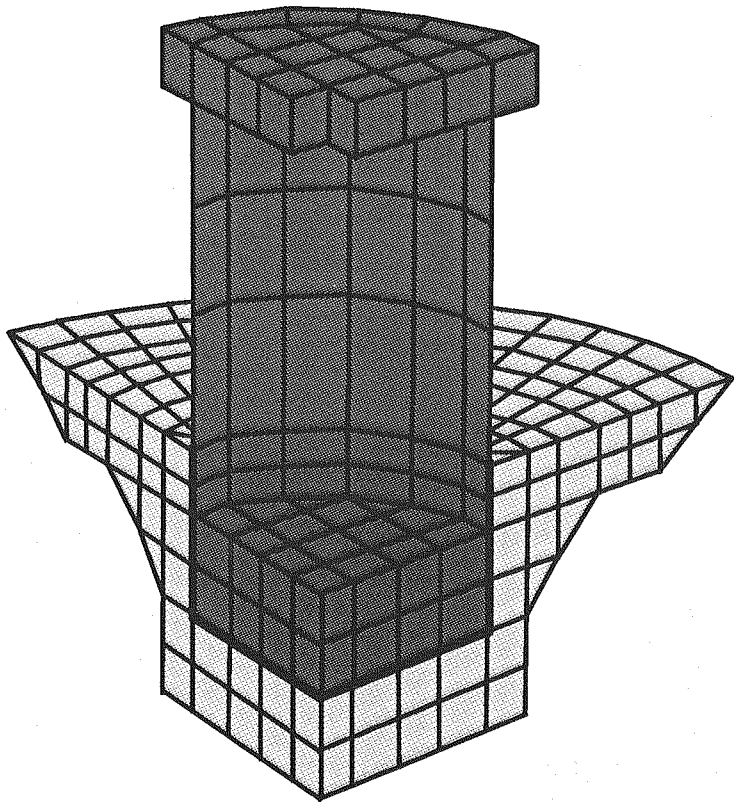

Figure 9. Three-dimensional quarter model (SASSI)

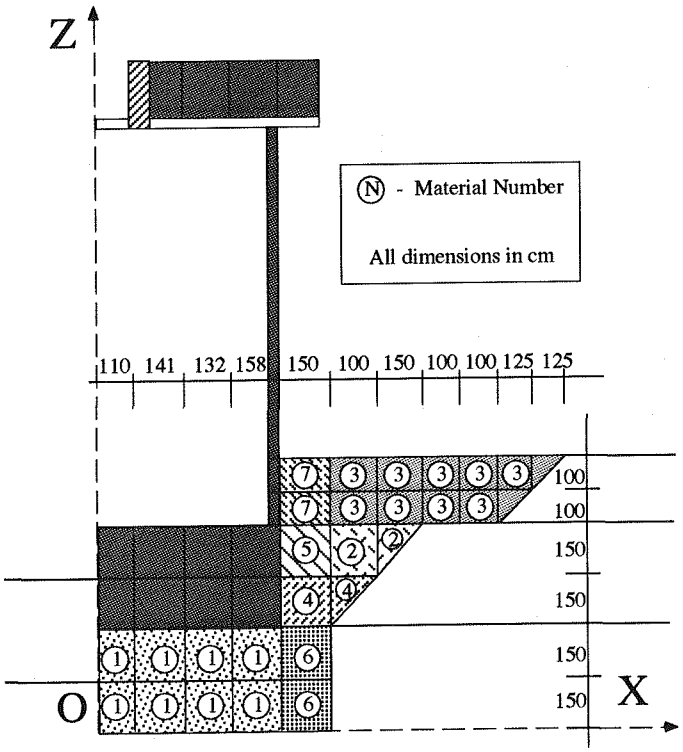

Figure 10. Discretization of the structure and the backfill into finite elements.

Table 4. Soil properties used for dynamic analysis in D2 direction.

Material Type	Unit weight g/cm^3	Poisson ratio	FVT Event 950530		Event 940120		Event 950501	
			Shear wave velocity m/s	Damping ratio %	Shear wave velocity m/s	Damping ratio %	Shear wave velocity m/s	Damping ratio %
1	2.42	0.48	250	5	100	5	100	5
2	2.39	0.48	300	2	300	2	300	2
3	2.33	0.38	300	2	300	2	300	2
4	2.39	0.48	225	2	225	2	200	4
5	2.42	0.48	225	2	225	2	200	4
6	2.42	0.48	225	2	225	2	200	4
7	2.33	0.38	225	2	100	2	100	4

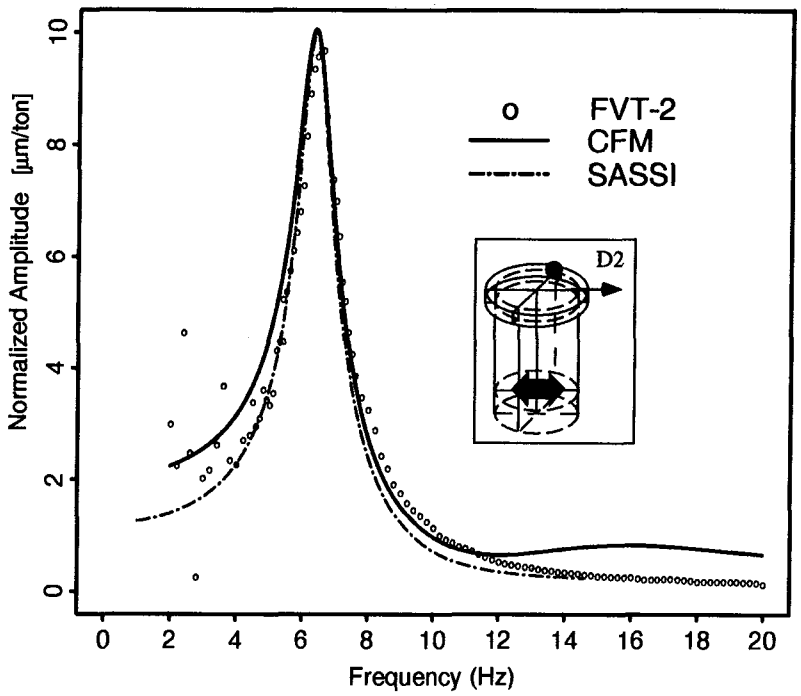

Figure 11. Simulation of FVT-2 with CFM and SASSI

While the SASSI analysis required detailed information about the site properties and elaborate finite element discretization, the sway-rocking model produced satisfactory results with only the backfill characteristics as input. This illustrates the advantage of the CFM as flexible and easily applicable for fast assessment of dynamic response of embedded structures.

Dynamic response to larger earthquakes

In order to simulate properly the response of the soil-structure system during larger earthquakes, account had to be taken of the weakening of the soil support. In each case, the properties of the backfill zone were parametrically varied and identified by comparison of recorded and calculated structural response.

Modification of the Parameters of the Sway-Rocking Model

The soil coefficients of the sway-rocking model were adjusted to fit the recorded response by a trial and error procedure, developed by Ganev et al. (1995a). The best-fit values of the soil stiffness and dashpot coefficients for all the analyzed earthquake records are plotted against the peak ground velocity in Figure 12.

These empirical relations are similar to the ones derived by Ganev et al. (1995a) using data from a model structure built on a soft soil site in Chiba, Japan. A general decreasing of the soil stiffness with increasing of the peak ground velocity is evident in both cases. It should be pointed out, however, that in the case of the Chiba tower, larger earthquake records were

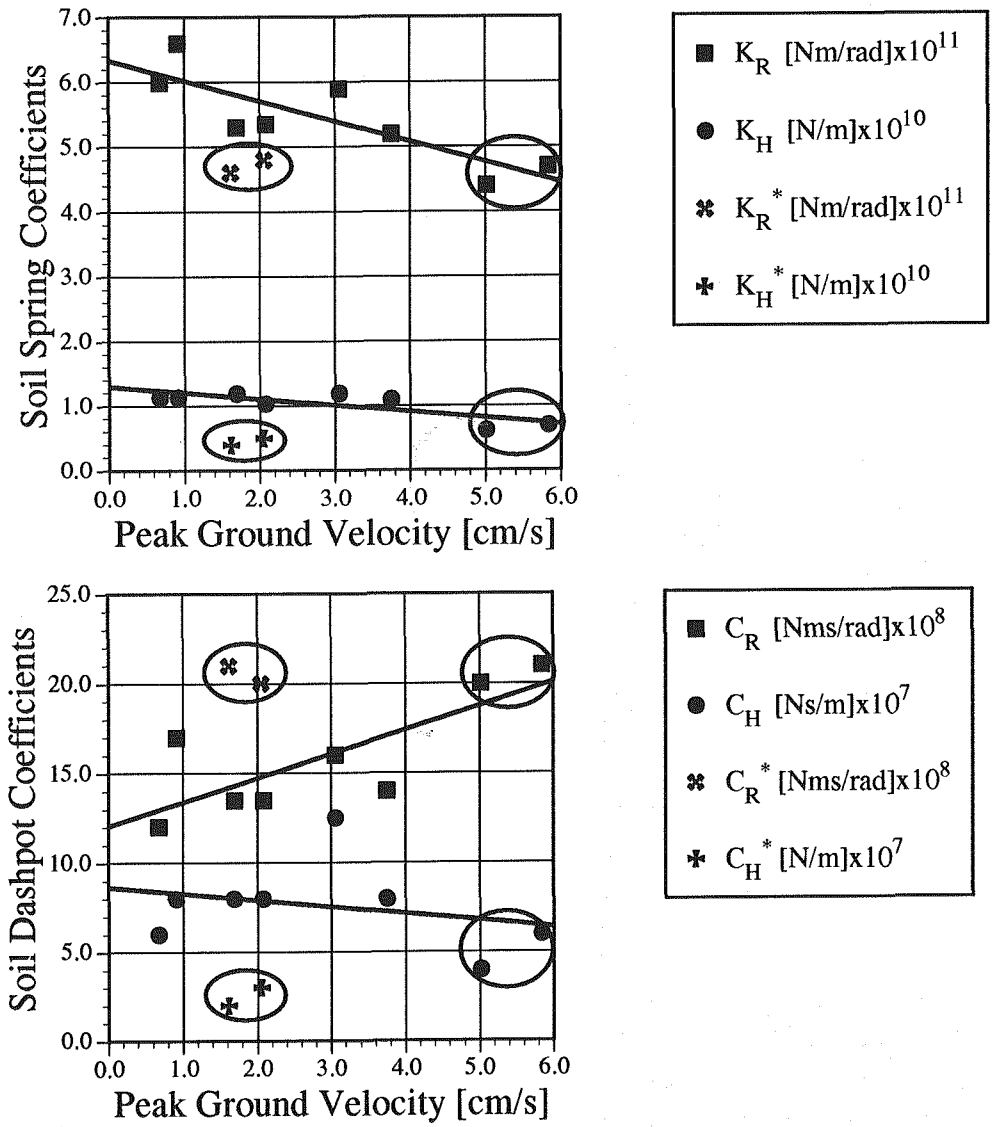

Figure 12. Empirical relations betveen the peak ground velocity and the parameters of the sway-rocking model

available and separation of structure from the soil was detected. Since no separation has been proven at the stiff soil, it follows, that the mechanism of soil stiffness degradation is different. As it was previously mentioned, local nonlinear effects are suspected to have caused this phenomenon.

The rocking damping coefficient at the soft soil has exhibited decrease due to separation, while in the Hualien case, a general increase is observed in accordance with the existing theory. However, no conclusive explanation can be offered at this time for the decreasing of the sway dashpot constant at the stiff soil site.

The values denoted with superscript (*) in Figure 12 are from Event 950502. The size of this earthquake is commensurate with the moderate Events 940120 and 940605, but it occurred

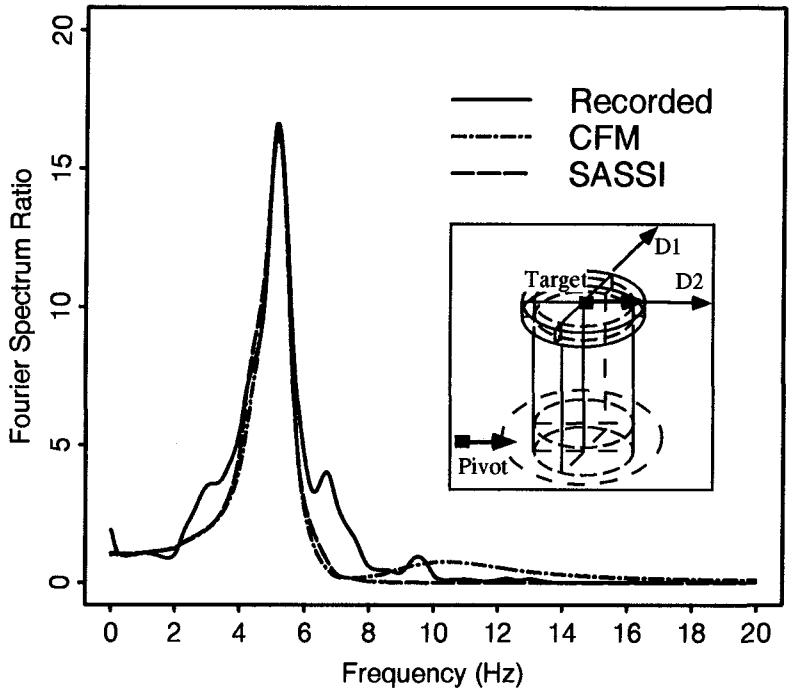

Figure 13. Simulation of the D2 component of Event 950501 with CFM and SASSI

within a day after the larger Event 950501 (c.f. Table 2). For reference, the points corresponding to Event 950501 are also encircled in Figure 12. It can be observed, that the best-fit values for Event 950502 are closer to those of the preceding stronger earthquake rather that to those of the other similar events. Apparently the soil stiffness remained weakened for some time after the occurrence of Event 950501. As no newer data are available, the present status of the soil support can not be evaluated. Considering, however, the values corresponding to Event 940120 and the following smaller Event 940530 it can be concluded, that the effect is generally reversible with time. The same phenomenon was observed by Ganev et al. (1995a) at the soft soil site in Japan. In that case, the analyzed data showed that the degradation of the soil stiffness was, in general, reversed. It is interesting to point out that the rocking damping coefficient at the Hualien site preserved a higher value for the time period while the stiffness was lower.

Modification of the Parameters of the Finite Element Model

Monitoring the alteration of the springs of the sway-rocking model gives a general idea of the decreasing of the soil stiffness. At the same time, the analysis with SASSI enables a more precise assessment with regard to which particular backfill region undergoes changes during earthquakes. Compared to the model used for small strain level, the model which fits best the response of the moderate Event 940120 has softer elements of type 1 and type 7 (Figure 10), which are in zones, where the local stress concentration is likely to be the highest, considering the rocking motion. For the larger Event 950501 the stiffness of the whole annular region decreases (Table 4). This supports the supposition that the soil stiffness degradation is caused by

local nonlinear effects.

A good agreement between numerical analysis and recorded response was achieved for all the studied earthquakes. An example of the simulation of the D2 component of Event 950501 is presented in Figure 13. It compares the recorded and calculated Fourier spectrum ratios between the free field and the top of the structure.

CONCLUSIONS

The dynamic behavior of a nuclear reactor containment model in Hualien, Taiwan was investigated, using data from forced vibration tests (FVT), microtremor observations and earthquake records. It was demonstrated that microtremor observations can be a good alternative to forced vibration tests in the small strain range. A shift of the predominant frequency of the soil-structure system during earthquakes was observed. This phenomenon signifies degradation of the soil stiffness under large dynamic loads.

The response of the containment model to FVT and earthquakes was simulated successfully with a sway-rocking model, whose soil parameters were evaluated on the basis of the Continuum Formulation Method (CFM). Empirical relations between the peak ground velocity of different earthquakes and the soil stiffness and damping coefficients of this model was derived. It was used to demonstrate that the soil stiffness remained weakened for certain time after a large earthquake and the rocking dashpot coefficient remained higher for the same period of time.

A comparison with the results of Ganev et al. (1995a) from analysis of a rigid tower on a soft soil site in Japan shows very similar phenomena. There is, however, some difference in the mechanism of soil stiffness degradation. In the case of the soft soil, separation of soil from structure was detected and proven to be a more influential factor than nonlinearity. The weakening of the soil stiffness, observed at the stiff soil site is attributed to local nonlinear effects.

Dynamic analysis was performed also with the Finite Element Method, using the program SASSI with the flexible volume substructuring approach. This model produced a very good agreement with the recorded response and was used to investigate which zones of the backfill undergo changes during earthquakes.

Comparing the backfill properties used to achieve best-fit results with the two numerical models, it was concluded, that the Continuum Formulation Method tends to underestimate the soil stiffness. The reason for this tendency was found in the theoretical basis of the method. Despite this shortcoming, the satisfactory results achieved with the CFM show that it has the advantage of being flexible and easily applicable for fast assessment of dynamic response of embedded structures.

REFERENCES

EPRI (1987). *Proceedings: EPRI/NRC/TPC Workshop on Seismic Soil-Structure Interaction Analysis Techniques Using Data from Lotung, Taiwan*, Palo Alto, California.

Ganev, T., F. Yamazaki, and T. Katayama (1995a). Observation and numerical analysis of soil-structure interaction of a reinforced concrete tower. *Earthquake Engineering and Structural Dynamics* **24**, 491-503.

Ganev, T., F. Yamazaki, T. Katayama and T. Ueshima (1995b). Soil-Structure Interaction of a Containment Model in Hualien, Taiwan. *Proceedings of the Twenty-third JSCE Earthquake Engineering Symposium*, pp. 397-400, Tokyo, Japan.

Harada, T., K. Kubo and T. Katayama (1981). Dynamic soil-structure interaction analysis by Continuum Formulation Method. *Report of the Institute of Industrial Science* **29**, University of Tokyo, Japan.

Kokusho, T., K Nishi, T. Okamoto, T. Kataoka, Y. Tanaka, K. Kudo, H. T. Tang and Y. H. Cheng (1993). Geotechnical investigation in the Hualien Large Scale Seismic Test project. *Transactions of the Twelfth International Conference on Structural Mechanics in Reactor Technology*, Vol. K1, Stuttgart, Germany.

Kokusho, T., K. Kudo, T. Okamoto, Y. Tanaka, T. Kawai, Y. Sawada, H. Yajima and K. Suzuki (1994). Soil-structure interaction research of a large-scale model structure at Hualien, Taiwan (Part 1). *Proceedings of the Ninth Japan Earthquake Engineering Symposium*, Vol. 2, pp. 1369-1374, Tokyo, Japan.

Lysmer, J. et al. (1988) SASSI, A System for Analysis of Soil-Structure Interaction, User's Manual.

Morisita, H., H. Tanaka, N. Nakamura, T. Kobayashi, S. Kan, H. Yamaya and H. T. Tang (1993). Forced vibration test of the Hualien Large Scale SSI model. *Transactions of the Twelfth International Conference on Structural Mechanics in Reactor Technology*, Vol. K02/1, pp. 37-42, Stuttgart, Germany.

Tanaka H., T. Sugiyama, T. Kobayashi and H. Yamaya (1994). Forced vibration test of the Hualien Large Scale SSI model (Part 2). *Proceedings of the Ninth Japan Earthquake Engineering Symposium*, Vol. 2, pp. 1387-1392, Tokyo, Japan. (In Japanese).

Tang, H. T., J. Stepp, et al. (1991). The Hualien Large-Scale Seismic Test for soil-structure interaction research. *Transactions of the Eleventh International Conference on Structural Mechanics in Reactor Technology*, Vol. K, pp. 69-74, Tokyo, Japan.

Tang, H. T. and N. Nakamura (1995). Analysis of the forced vibration test of the Hualien Large Scale Soil-Structure Interaction model using a Flexible Volume Substructuring Method. *Proceedings of the Third JSME/ASME Joint International Conference on Nuclear Engineering, (ICONE-3)*, Vol. 4, pp. 2053-2058, Kyoto, Japan.

Veletsos, A. and K. Dotson (1988). Horizontal impedances for radially inhomogeneous viscoelastic soil layers. *Earthquake Engineering and Structural Dynamics*, **16**, 947-966.

Yamazaki, F., L. Lu and T. Katayama (1992). Orientation error estimation of buried seismographs in array observation. *Earthquake Engineering and Structural Dynamics*, **21**, 679-694.